Electronic Supplementary Information (ESI) for

Hexavacant γ-Dawson-type phosphotungstates supporting an edge-sharing bis(square-pyramidal) $\{O_2M(\mu_3\text{-}O)_2(\mu\text{-}OAc)MO_2\}$ core ($M = Mn^{2+}$, Co^{2+}, Ni^{2+}, Cu^{2+}, or Zn^{2+})†

Kosuke Suzuki,* [a,b] Takuo Minato,[a] Naoto Tominaga,[a] Ichiro Okumo,[a] Kentaro Yonesato,[a] Noritaka Mizuno[a] and Kazuya Yamaguchi* [a]

[a]*Department of Applied Chemistry, School of Engineering, The University of Tokyo, 7-3-1 Hongo, Bunkyo-ku, Tokyo 113-8656, Japan.*

E-mail: ksuzuki@appchem.t.u-tokyo.ac.jp, kyama@appchem.t.u-tokyo.ac.jp

[b]*Precursory Research for Embryonic Science and Technology (PRESTO), Japan Science and Technology Agency (JST), 4-1-8 Honcho, Kawaguchi, Saitama 332-0012, Japan.*

Table S1. BVS values of metal atoms and metal atoms for **Mn2**, **Co2**, **Ni2**, **Cu2**, and **Zn2**

	Mn2	**Co2**	**Ni2**	**Cu2**	**Zn2**
M1	2.08	1.96	1.95	2.09	2.05
P1	4.81	4.91	4.78	4.82	4.83
W1	5.98	6.73	6.12	5.93	6.21
W2	6.44	7.08	5.69	6.35	6.26
W3	6.18	5.71	7.66	6.63	6.61
W4	6.23	5.84	6.34	6.42	6.25
W5	5.97	6.63	5.75	6.31	6.44
W6	6.45	6.01	6.87	6.20	6.62
O1	1.85	2.06	1.95	2.02	1.89
O2	1.98	1.81	1.94	1.97	2.03
O3	1.97	1.95	1.94	2.00	1.95
O4	1.67	2.09	1.86	1.72	1.75
O5	1.84	1.87	1.65	1.48	1.88
O6	1.61	1.50	1.79	2.10	1.60
O7	1.81	1.48	1.56	1.70	1.69
O8	2.10	2.18	2.20	2.13	2.17
O9	2.00	2.00	2.01	2.00	2.03
O10	1.99	2.04	2.08	2.05	2.01
O11	2.04	2.13	2.05	2.12	2.09
O12	1.89	1.90	1.91	1.91	1.91
O13	1.86	1.82	1.77	1.92	1.79
O14	1.74	1.90	1.86	1.80	1.88
O15	1.94	1.97	1.96	2.02	2.00
O16	2.16	2.19	1.98	2.23	2.09
O17	2.02	2.04	2.52	2.10	2.08
O18	1.99	2.07	2.01	1.97	1.93
O19	2.19	2.23	2.22	2.19	2.23
O20	2.10	2.10	2.12	2.08	2.11
O21	1.60	1.97	1.46	1.80	1.70
O22	2.00	1.73	2.31	1.80	2.09

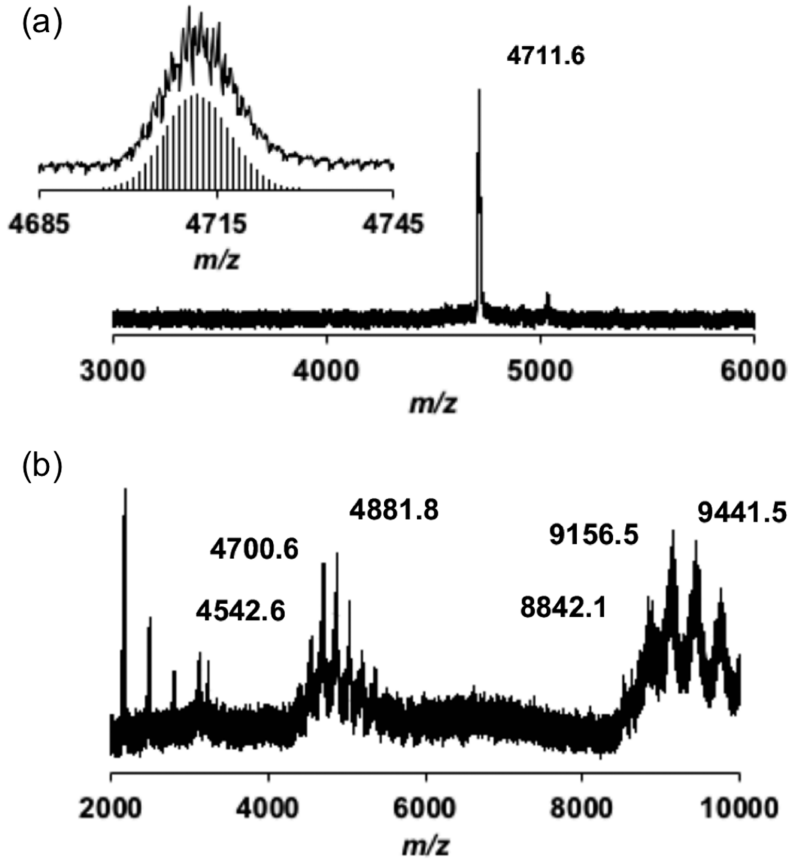

Fig. S1 Positive-ion CSI-mass spectra of (a) the reaction solution of **I**, $Mn(OAc)_2$, and TBAOH in acetonitrile, and (b) the reaction solution of **I** and $Mn(OAc)_2$ in dichloromethane.

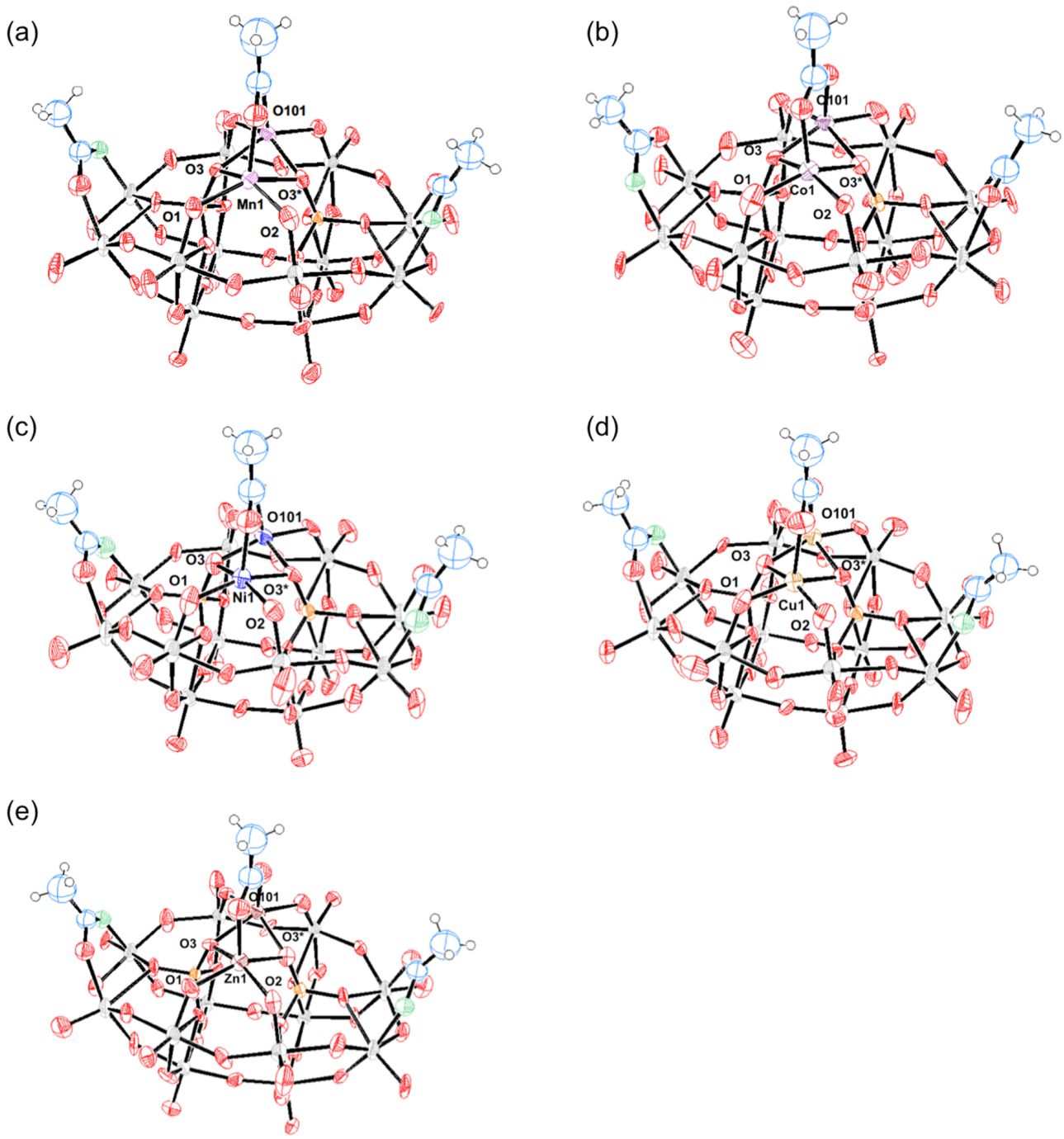

Fig. S2 ORTEP representations of the anion part of (a) **Mn2**, (b) **Co2**, (c) **Ni2**, (d) **Cu2**, and (e) **Zn2** with thermal ellipsoids drawn at the 50% probability level.

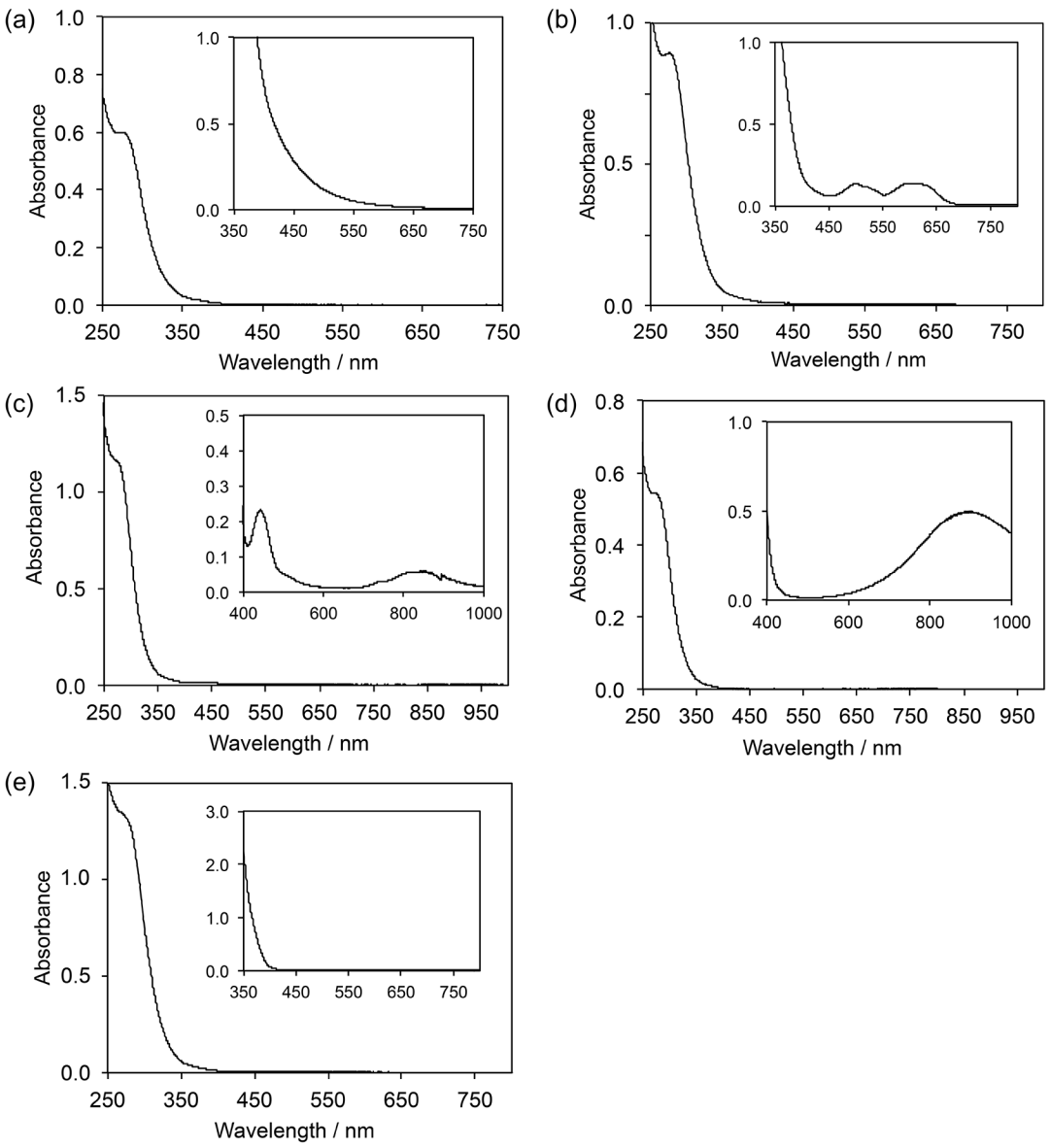

Fig. S3 UV-vis spectra of (a) **Mn2** (2.0×10^{-5} M, Inset: 8.2×10^{-4} M), (b) **Co2** (2.5×10^{-5} M, Inset: 1.0×10^{-3} M), (c) **Ni2** (3.6×10^{-5} M, Inset: 1.8×10^{-3} M), (d) **Cu2** (1.9×10^{-5} M, Inset: 5.4×10^{-3} M), and (e) **Zn2** (4.0×10^{-5} M, Inset: 2.0×10^{-3} M) in acetonitrile.

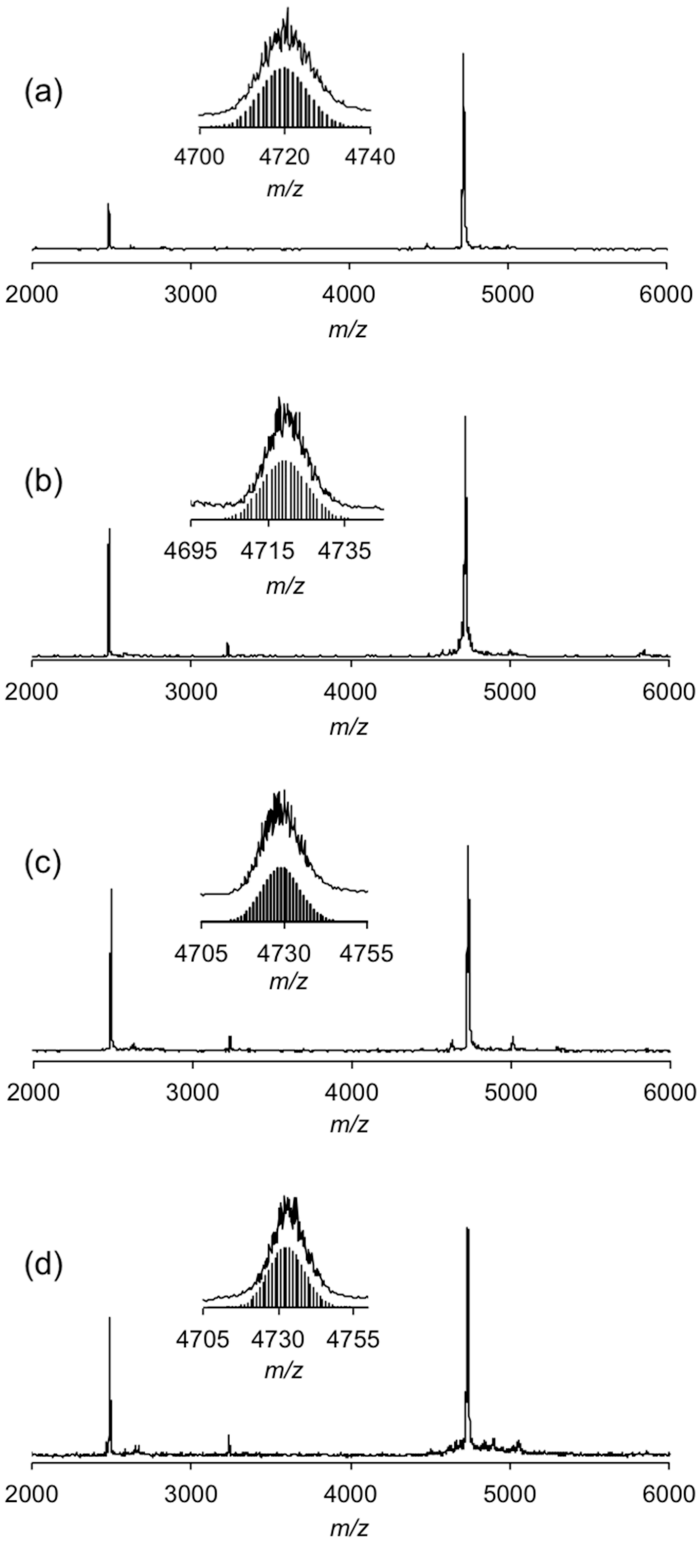

Fig. S4 Positive-ion CSI-mass spectra of (a) **Co2**, (b) **Ni2**, (c) **Cu2**, and (d) **Zn2** in acetonitrile.

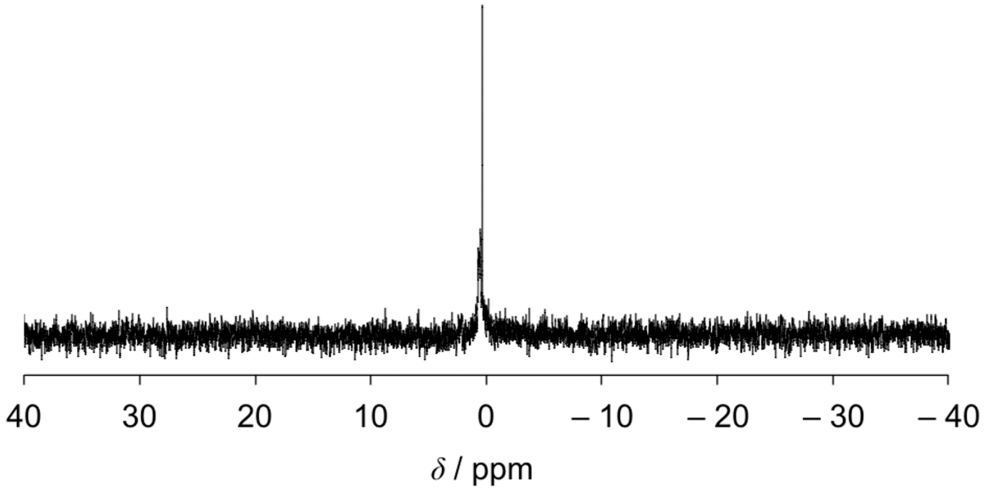

Fig. S5 ^{31}P NMR spectrum of **Zn2** in dichloromethane-d_2.

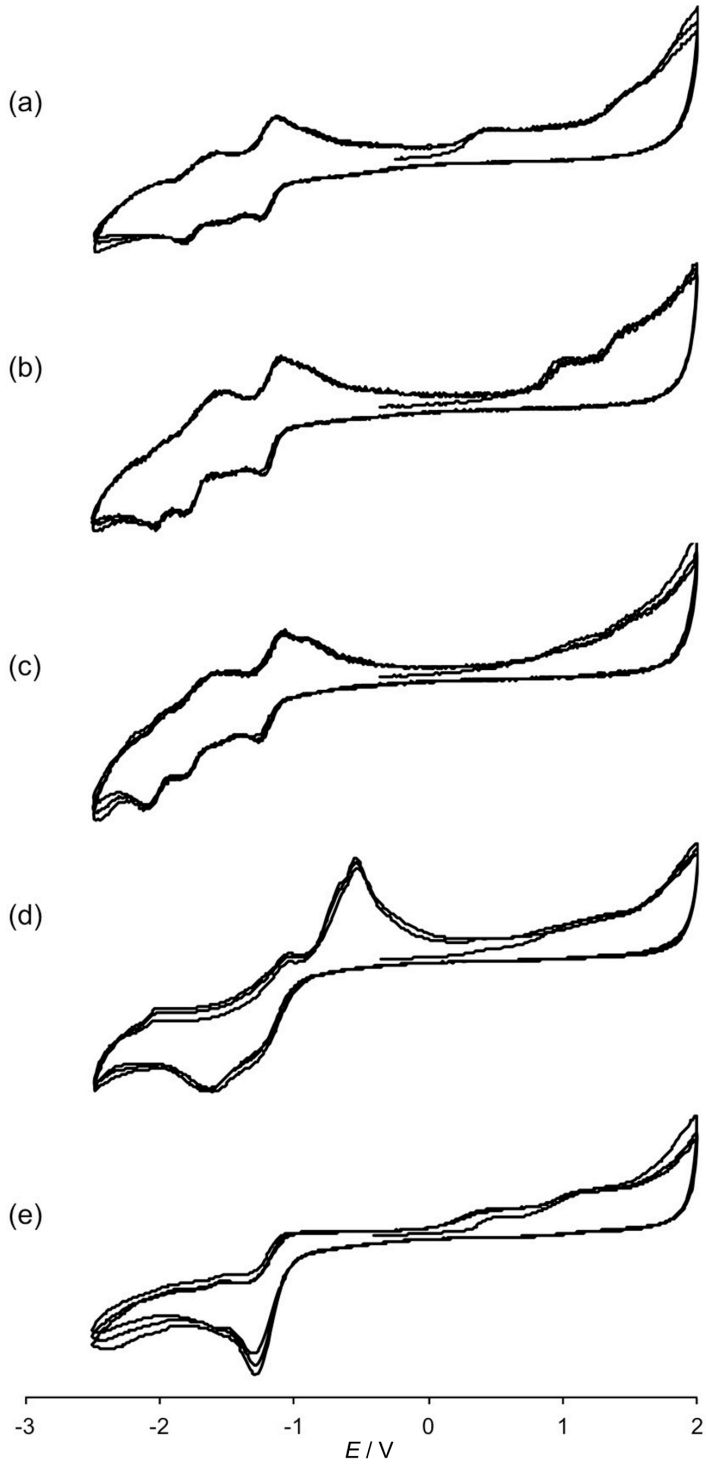

Fig. S6 Cyclic voltammogram of (a) **Mn2**, (b) **Co2**, (c) **Ni2**, (d) **Cu2**, and (e) **Zn2**.

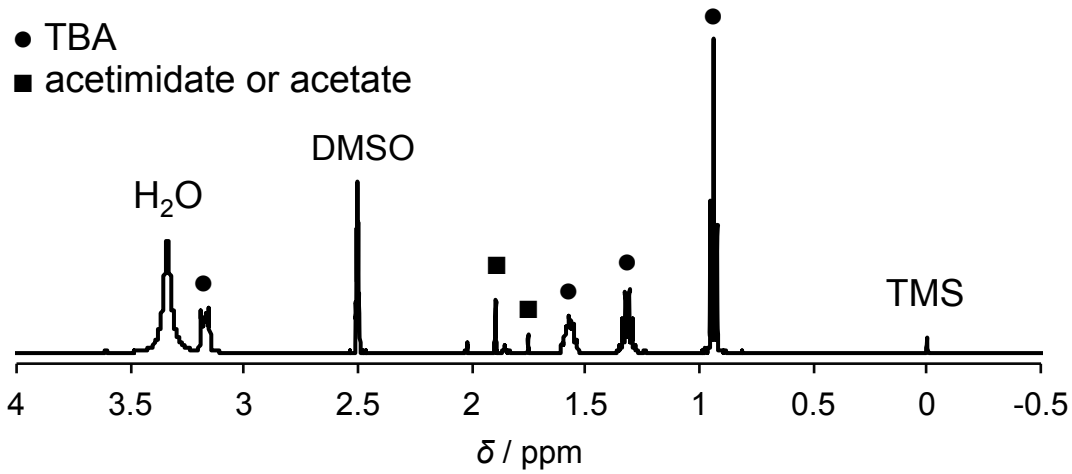

Fig. S7 ^{1}H NMR spectrum of **Zn2** in dimethyl sulfoxide-d_6.

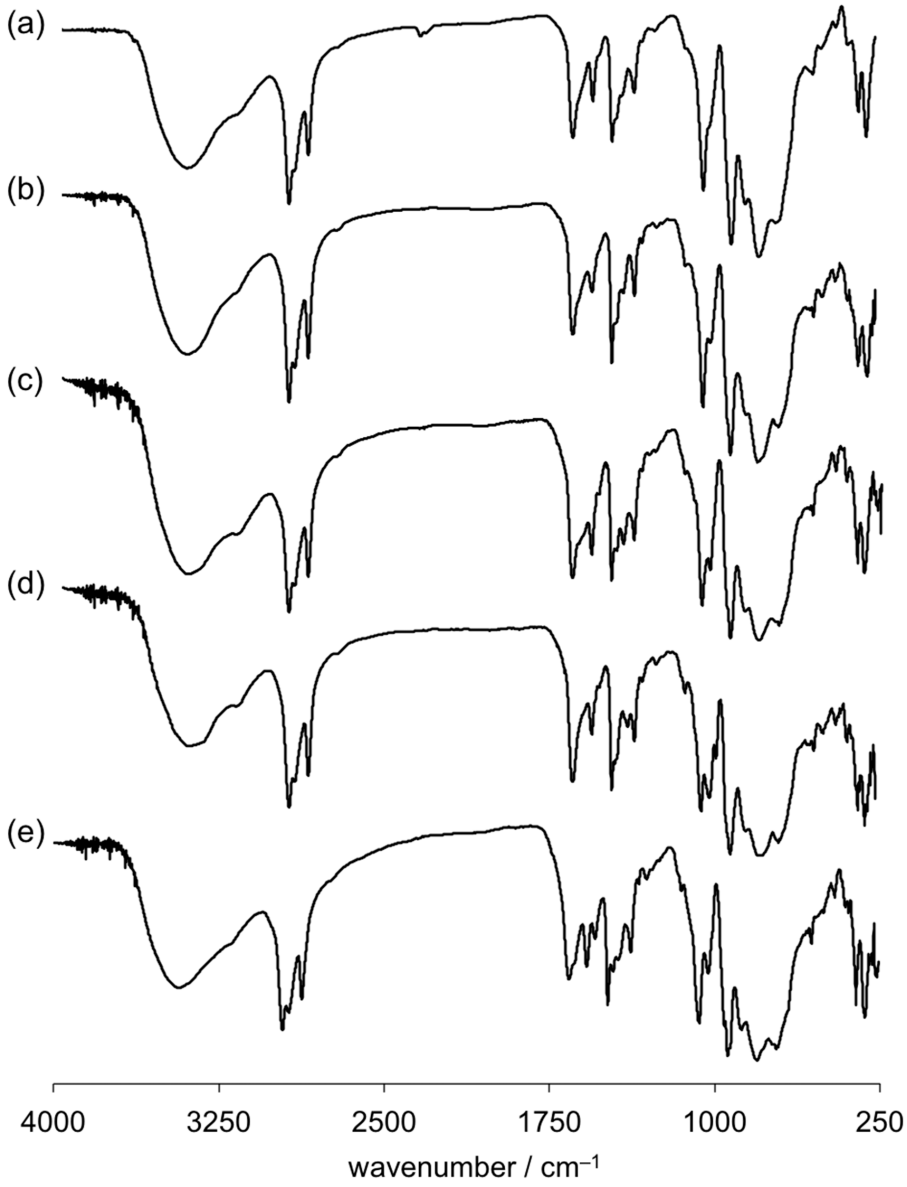

Fig. S8 IR spectra of (a) **Mn2**, (b) **Co2**, (c) **Ni2**, (d) **Cu2**, and (e) **Zn2**.